symmetry

IMPACT FACTOR 2.7

CITESCORE 4.9

Article

Gamow–Teller Beta Decay and Pseudo-SU(4) Symmetry

Piet Van Isacker, Alejandro Algora, András Vitéz-Sveiczer, Gábor Gyula Kiss, Sonja Elena Agata Orrigo, Berta Rubio and Pablo Aguilera

Special Issue

Role of Symmetries in Nuclear Physics

Edited by

Prof. Dr. Peter Otto Hess

MDPI

https://doi.org/10.3390/sym15112001

symmetry

MDPI

Article

Gamow–Teller Beta Decay and Pseudo-SU(4) Symmetry

Piet Van Isacker [1], Alejandro Algora [2,3,*], András Vitéz-Sveiczer [3,4], Gábor Gyula Kiss [3], Sonja Elena Agata Orrigo [2], Berta Rubio [2] and Pablo Aguilera [5,6]

1 Grand Accélérateur National d'Ions Lourds (GANIL), CEA/DSM-CNRS/IN2P3, Bvd Henri Becquerel, F-14076 Caen, France; isacker@ganil.fr
2 Instituto de Física Corpuscular, E-46980 Paterna, Spain; rubio@ific.uv.es (B.R.)
3 Institute for Nuclear Research (Atomki), H-4001 Debrecen, Hungary; sveiczer.andras@atomki.hu (A.V.-S.); ggkiss@atomki.hu (G.G.K.)
4 Doctoral School of Physics, University of Debrecen, H-4001 Debrecen, Hungary
5 Dipartimento di Fisica e Astronomia, Università degli Studi di Padova, I-35131 Padova, Italy; pabloantonio.aguilerajorquera@unipd.it
6 Istituto Nazionale di Fisica Nucleare (INFN), Sezione di Padova, I-35131 Padova, Italy
* Correspondence: algora@ific.uv.es

Abstract: We report on recent experimental results on β decay into self-conjugate ($N = Z$) nuclei with mass number $58 \leq A \leq 70$. Super-allowed β decays from the $J^\pi = 0^+$ ground state of a $Z = N + 2$ parent nucleus are to the isobaric analogue state through so-called Fermi transitions and to $J^\pi = 1^+$ states by way of Gamow–Teller (GT) transitions. The operator of the latter decay is a generator of Wigner's SU(4) algebra and as a consequence GT transitions obey selection rules associated with this symmetry. Since SU(4) is progressively broken with increasing A, mainly as a consequence of the spin–orbit interaction, this symmetry is not relevant for the nuclei considered here. We argue, however, that the *pseudo*-spin–orbit splitting can be small in nuclei with $58 \leq A \leq 70$, in which case nuclear states exhibit an approximate pseudo-SU(4) symmetry. To test this conjecture, GT decay strength is calculated with use of a schematic Hamiltonian with pseudo-SU(4) symmetry. Some generic features of the GT β decay due to pseudo-SU(4) symmetry are pointed out. The experimentally observed GT strength indicates a restoration of pseudo-SU(4) symmetry for $A = 70$.

Keywords: Gamow–Teller β decay; pseudo-SU(4) symmetry; odd–odd $N = Z$ nuclei

Citation: Van Isacker, P.; Algora, A.; Vitéz-Sveiczer, A.; Kiss, G.G.; Orrigo, S.E.A.; Rubio, B.; Aguilera, P. Gamow–Teller Beta Decay and Pseudo-SU(4) Symmetry. *Symmetry* **2023**, *15*, 2001. https://doi.org/10.3390/sym15112001

Academic Editor: Peter Otto Hess

Received: 2 October 2023
Revised: 24 October 2023
Accepted: 26 October 2023
Published: 31 October 2023

1. Introduction

Allowed β decays from the $J^\pi = 0^+$ ground state of a $Z = N + 2$ parent nucleus can proceed through two different processes: either through a super-allowed Fermi transition to the isobaric analogue $J^\pi = 0^+$ state in the $N = Z$ daughter nucleus or to $J^\pi = 1^+$ states by way of Gamow–Teller (GT) transitions. In both cases, a proton is transformed into a neutron with the emission of a positron and an electron-neutrino. A Fermi transition can be viewed as a change of the isospin state of a nucleon with other quantum numbers remaining the same, whereas a GT transition involves the simultaneous flipping of the nucleon's spin and isospin.

The GT transition operator is a generator of Wigner's SU(4) (or supermultiplet) algebra [1], and, as such, GT transitions obey the selection rules dictated by this symmetry. While SU(4) symmetry might be a reasonable approximation in light (i.e., p-shell) nuclei, it becomes strongly broken as the mass number A of the nucleus increases, mainly as a consequence of the spin–orbit interaction. Many years ago, it was argued, however, that a much weaker *pseudo*-spin–orbit interaction exists in nuclei. With reference to the original papers [2,3] for a general definition of pseudo-spin symmetry, in the nuclei of interest here, it amounts to treating the $1p_{1/2}$, $1p_{3/2}$ and $0f_{5/2}$ orbitals as a pseudo-sd shell. It then becomes natural to assume invariance under transformations in pseudo-spin and isospin space, that is, to assume that the nuclear Hamiltonian exhibits a pseudo-SU(4) symmetry.

The purpose of this contribution is to present a summary of recently obtained experimental distributions of GT strength in the $58 \leq A \leq 70$ mass region and to compare these results to the predictions of a schematic model with pseudo-SU(4) symmetry.

We start in Section 2 with a brief review of experimental results concerning GT β decay into $N = Z$ nuclei. In Section 3, a formal definition is given of the GT transition operator together with various expressions of its matrix elements. This is followed by a discussion of Wigner's SU(4) symmetry and its extension to pseudo-SU(4) in Sections 4 and 5, respectively. The GT β decay of nuclei with two valence nucleons is discussed in detail in Section 6 and applied to the decay of ^{18}Ne and ^{58}Zn as examples of GT transitions ruled by SU(4) and pseudo-SU(4) symmetry, respectively. The latter approach is extended to $A = 62$, 66 and 70 in Section 7. Finally, a summary of this work is presented in Section 8.

2. A Review of Experimental Results

In this section, we discuss briefly the latest experimental results regarding four exotic β decays of interest (see Figure 1). These decays have been studied at radioactive-beam facilities of the fragmentation type, like GANIL (France) [4], GSI (Germany) [5], and RIKEN Nishina Center (Japan) [6]. The production of these exotic nuclei is more challenging with increasing mass. These β decays are not only of interest for nuclear structure but they are also relevant for explosive nucleosynthesis, in particular for the astrophysical rp-process [7,8].

Results of the β-decay study of ^{58}Zn into ^{58}Cu have been recently published by Kucuk et al. [9]. The nucleus ^{58}Zn was produced in GANIL using a primary beam of ^{64}Zn^{29+} at 79 MeV/nucleon impinging in a natural nickel target with a thickness of 236 mg/cm^2. The reaction fragments were selected in the LISE3 separator [10], identified using the ToF–$B\rho$ for the (A/q) and the ΔE signal for the Z identification, and implanted in a double-sided silicon strip detector (DSSD). The implantation detector was surrounded by three EXOGAM clovers and a smaller EUROBALL clover of high-purity germanium detectors (HPGe) to detect the β-delayed γ rays. The β decay of ^{58}Zn is dominated by a super-allowed Fermi transition to the isobaric analog state at 203 keV excitation. Two weaker GT transitions to the first 1^+ state (the ground state) and to a level at 1051 keV excitation were also identified.

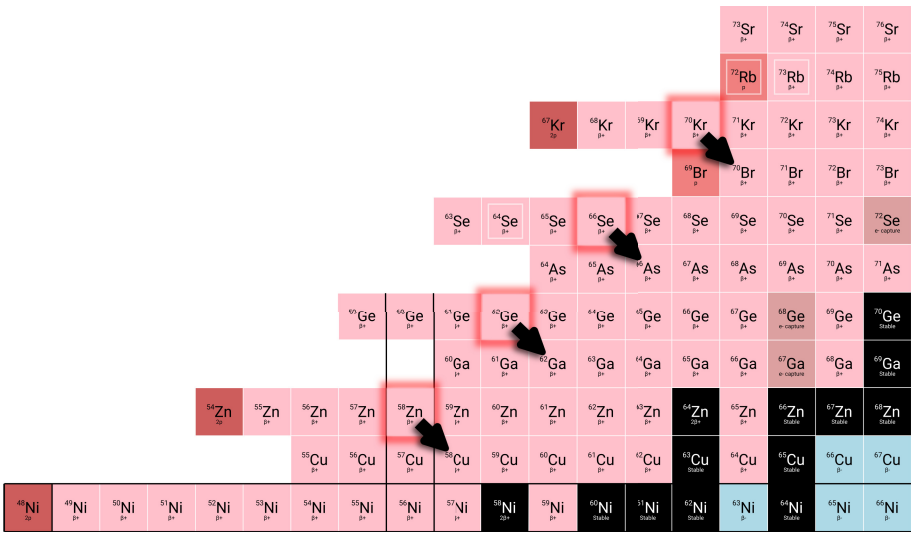

Figure 1. Part of the nuclide chart representing the position of the decays of interest. Figure created using the *Colourful Nuclide Chart* tool [11]. The decays of interest are marked with black arrows.

The other decays of interest, ^{62}Ge into ^{62}Ga, ^{66}Se into ^{66}As and ^{70}Kr into ^{70}Br have been recently studied at RIBF in RIKEN Nishina Center. These, together with other nuclei with $30 \leq Z \leq 36$, were produced by the fragmentation of a 345 MeV/nucleon ^{78}Kr primary beam with average intensities of 40 pnA impinging on a 5 mm thick ^{9}Be target. The parent nuclei of interest were produced in four different settings centred on ^{64}Se, ^{65}Br, ^{66}Se, and

^{70}Kr. The fragmentation reaction products were separated using the BigRIPS fragment separator [12]. As in the previous case the identification of particles with the atomic number (Z) and the mass-to-charge ratio (A/q) was performed on the basis of the $\Delta E - ToF - B\rho$ method, in which the energy loss (ΔE), time of flight (ToF), and magnetic rigidity $(B\rho)$ were measured using detectors installed along the BigRIPS fragment separator. In the study, the WAS3ABi implantation detector [13], consisting of three layers of highly-segmented DSSDs, was used. This detector was surrounded by the EURICA spectrometer [14], which consisted of 84 HPGe crystals arranged in twelve clusters at a nominal distance of 22 cm from the centre of WAS3ABi. The absolute peak efficiency was found to be ∼8% at 1332 keV.

The β decay of ^{62}Ge into ^{62}Ga was first studied in detail at GSI [15], establishing a level scheme that contained six states. This level scheme was revisited in a recent study by Orrigo et al. [16] performed at RIKEN as described earlier. Four of the states seen in Ref. [15] were confirmed in Orrigo's work [16], and a much richer level scheme was deduced. Eight new γ rays were identified for the first time in the RIKEN experiment, and the four strongest γ transitions seen by Grodner et al. [15] in the GSI experiment were confirmed. However, the $E_\gamma = 1247$ keV and $E_\gamma = 2414$ keV transitions identified by Grodner were not confirmed in Orrigo's study. Figure 2 shows the γ-ray energy spectrum for decay events correlated with ^{62}Ge implants measured at RIKEN. Based on the measured γ spectra, a new level scheme was constructed, containing twelve 1^+ states, with one state being assigned (1^+) only tentatively. In this last experiment, the half-life value of $t_{1/2} = 73.5(1)$ ms was also determined with higher precision than in earlier works. The new value is in agreement with Kucuk et al. [9] within the uncertainty of their value, thus settling the question of earlier conflicting values [15,17].

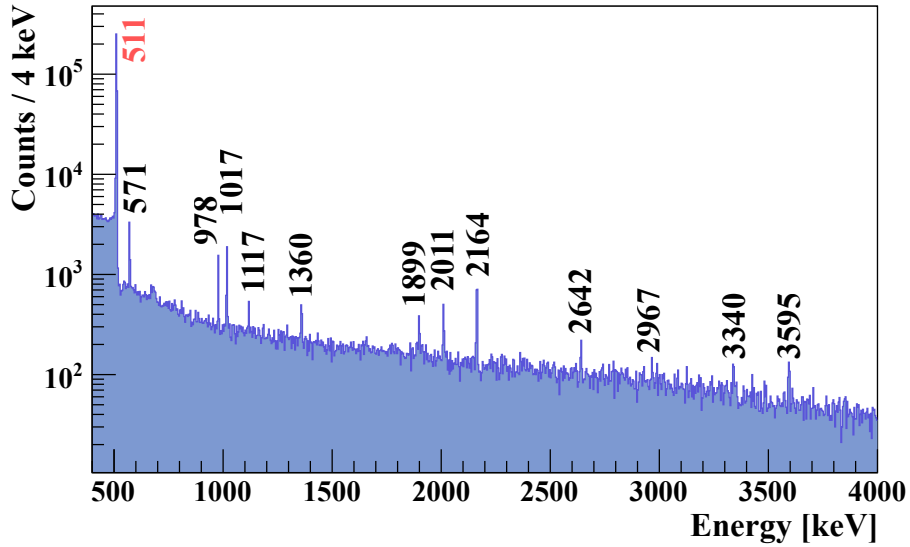

Figure 2. γ-Ray energy spectrum for decay events correlated with ^{62}Ge implants.

For the ^{66}Se into ^{66}As case, a publication is in preparation [18] and we will only present the β-strength results deduced from this work [19] in comparison with theory.

The β decay of the ^{70}Kr isotope was studied in Sveiczer et al. [20] from the RIKEN data of the same campaign. The level scheme of the ^{70}Br daughter isotope populated in the β decay of ^{70}Kr was established with eleven populated states below $E_{\text{exc}} = 3300$ keV and fifteen γ transitions identified for the first time (see Figure 3). They are shown in Figure 4. Previously, no levels populated in the β decay were known with the exception of the 2^+ state at 933 keV, which was also known from in-beam studies [21,22]. The half-life of the decay was also determined from implant –β-decay correlations with increased precision, providing a value of $t_{1/2} = 45.19(14)$ ms.

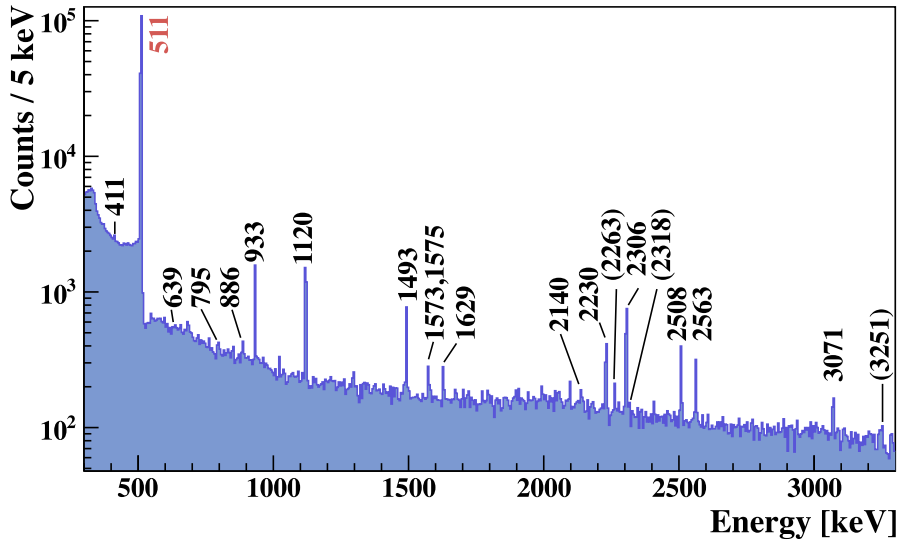

Figure 3. γ-Ray energy spectrum for decay events correlated with ^{70}Kr implants [20].

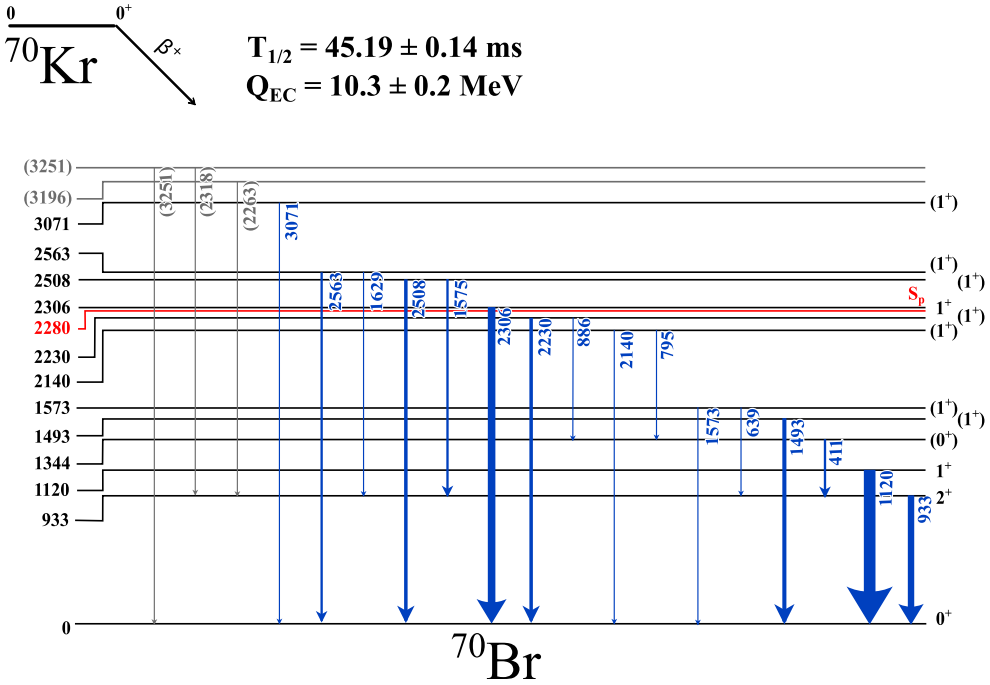

Figure 4. Partial level scheme of ^{70}Br derived from the β decay of ^{70}Kr. The excitation energies and most probable spins and parities (J^π) of the observed states are indicated on the right-hand side of the levels. The arrow widths are proportional to absolute intensities of the γ rays. Tentatively assigned levels and their corresponding γ rays are labelled between brackets. S_p represents the one-proton separation energy [20].

An interesting common feature of the studied decays is that they do not show γ transitions between the identified 1^+ states. This indirectly confirms their $J^\pi = 1^+$ assignment based on the quasi-rule that $\Delta T = 0$ M1 transitions in self-conjugate nuclei are expected to be weaker by a factor of 100 than the average M1 transition strength [23]. This fact was already observed in the study of lighter $Z = N + 2$ decays [24].

3. The Gamow–Teller Operator and the Ikeda Sum Rule

The GT operator transforms as a rank-one tensor (i.e., vector) in spin and in isospin space. Conventionally, it is taken to be

$$\sum_{k=1}^{A} M_{\mu}^{\pm}(k) = \sum_{k=1}^{A} \sigma_{\mu}(k) t_{\pm}(k) = \frac{1}{\sqrt{2}} \sum_{k=1}^{A} \sigma_{\mu}(k) \tau_{\pm 1}(k), \tag{1}$$

where the summation is over the A nucleons in the nucleus, $\bar{\sigma}(k)$ and $\bar{\tau}(k)$ are the spin and isospin vectors and $t_{\pm}(k)$ are the isospin raising and lowering operators of nucleon k. For ease of notation the summation over k and the index k will be suppressed in the following, $\sum_k M_{\mu}^{\pm}(k) \rightarrow M_{\mu}^{\pm}$, etc. The total GT strength created by the operator (1) on an initial state $|\mathrm{i}\rangle$ is given by the sum [25]

$$S^{\pm}(\mathrm{i}) = \sum_{\mu=-1}^{+1} \sum_{\mathrm{f}} |\langle \mathrm{f}|M_{\mu}^{\pm}|\mathrm{i}\rangle|^2, \tag{2}$$

where the summation in f is over all possible final states. Because of the operator identity $[M_{\mu}^{+}, M_{\mu}^{-}] = -2T_z$, the summed GT $\beta^{\pm}$ strength satisfies the Ikeda sum rule [26]

$$S^{-}(\mathrm{i}) - S^{+}(\mathrm{i}) = 3(N - Z). \tag{3}$$

The reduced GT strength from an initial to a final state $|J_\mathrm{i} T_\mathrm{i} T_{z\mathrm{i}}\rangle \rightarrow |J_\mathrm{f} T_\mathrm{f} T_{z\mathrm{f}}\rangle$, where states are characterized by total angular momentum J, isospin T, and isospin projection T_z, is given by

$$B(\mathrm{GT}; J_\mathrm{i} T_\mathrm{i} T_{z\mathrm{i}} \rightarrow J_\mathrm{f} T_\mathrm{f} T_{z\mathrm{f}}) = \frac{1}{2J_\mathrm{i}+1} |\langle J_\mathrm{f} T_\mathrm{f} T_{z\mathrm{f}}||M^{\pm}||J_\mathrm{i} T_\mathrm{i} T_{z\mathrm{i}}\rangle|^2, \tag{4}$$

where the matrix element is reduced by the Wigner–Eckart theorem in angular momentum following the convention of Talmi [27]. The matrix element can be further reduced [28] by applying the Wigner–Eckart theorem in isospin, leading to

$$B(\mathrm{GT}; J_\mathrm{i} T_\mathrm{i} T_{z\mathrm{i}} \rightarrow J_\mathrm{f} T_\mathrm{f} T_{z\mathrm{f}}) = \frac{1}{2(2J_\mathrm{i}+1)} \begin{pmatrix} T_\mathrm{i} & 1 & T_\mathrm{f} \\ -T_{z\mathrm{i}} & T_{z\mathrm{i}} - T_{z\mathrm{f}} & T_{z\mathrm{f}} \end{pmatrix}^2 |\langle J_\mathrm{f} T_\mathrm{f}|||\bar{\sigma}\bar{\tau}|||J_\mathrm{i} T_\mathrm{i}\rangle|^2, \tag{5}$$

where the matrix element is now reduced in angular momentum J and isospin T.

The calculation of GT strength for a Hamiltonian with pseudo-spin symmetry requires matrix elements of the type

$$\langle LSJT|||(Y_\lambda \times \bar{\sigma})^{(1)} \bar{\tau}|||L'S'J'T'\rangle = \sqrt{3}\hat{J}\hat{J}' \begin{Bmatrix} L & S & J \\ L' & S' & J' \\ \lambda & 1 & 1 \end{Bmatrix} \langle LST||||Y_\lambda \bar{\sigma}\bar{\tau}||||L'S'T'\rangle, \tag{6}$$

with $\hat{x} = \sqrt{2x+1}$ and where the symbol in curly brackets is a nine-j coeffcient and $Y_{\lambda\mu}(\theta, \varphi)$ is a spherical harmonic of multipolarity λ [27]. The matrix element on the left-hand side of Equation (6) is reduced in J and T while that on the right-hand side is reduced in L, S and T. This formula will be applied for $\lambda = 0$ (the standard GT operator) and for $\lambda = 2$, which contributes to the pseudo-spin-transformed operator (see below). The reduced GT strength for the transition $|L_\mathrm{i} S_\mathrm{i} J_\mathrm{i} T_\mathrm{i} T_{z\mathrm{i}}\rangle \rightarrow |L_\mathrm{f} S_\mathrm{f} J_\mathrm{f} T_\mathrm{f} T_{z\mathrm{f}}\rangle$ is therefore

$$\begin{aligned} &B(\mathrm{GT}; L_\mathrm{i} S_\mathrm{i} J_\mathrm{i} T_\mathrm{i} T_{z\mathrm{i}} \rightarrow L_\mathrm{f} S_\mathrm{f} J_\mathrm{f} T_\mathrm{f} T_{z\mathrm{f}}) \\ &= \frac{3(2J_\mathrm{f}+1)}{2} \begin{pmatrix} T_\mathrm{i} & 1 & T_\mathrm{f} \\ -T_{z\mathrm{i}} & T_{z\mathrm{i}} - T_{z\mathrm{f}} & T_{z\mathrm{f}} \end{pmatrix}^2 \begin{Bmatrix} L_\mathrm{f} & S_\mathrm{f} & J_\mathrm{f} \\ L_\mathrm{i} & S_\mathrm{i} & J_\mathrm{i} \\ \lambda & 1 & 1 \end{Bmatrix}^2 |\langle L_\mathrm{f} S_\mathrm{f} T_\mathrm{f}||||Y_\lambda \bar{\sigma}\bar{\tau}||||L_\mathrm{i} S_\mathrm{i} T_\mathrm{i}\rangle|^2. \end{aligned} \tag{7}$$

4. Wigner's SU(4) Symmetry

Wigner [1] assumed that the nuclear Hamiltonian is spin as well as isospin independent,

$$[H, \sigma_\mu] = [H, \tau_\nu] = [H, \sigma_\mu \tau_\nu] = 0, \tag{8}$$

in which case the nuclear Hamiltonian has SU(4) symmetry. The n-nucleon eigenstates of this Hamiltonian can be classified according to

$$\begin{array}{ccccc} \mathrm{U}(4\Gamma) & \supset & \mathrm{U}(\Gamma) & \otimes & \mathrm{U}_{ST}(4) \\ \downarrow & & \downarrow & & \downarrow \\ [1^n] & & [\bar{h}] & & [\bar{h}'] \end{array}, \tag{9}$$

where Γ is the orbital dimension of the single-particle space, $\Gamma = \sum_l (2l+1)$, and 4Γ is the total dimension for neutrons and protons that takes care of the spin and isospin degrees of freedom. If the nucleons occupy an entire shell of the harmonic oscillator with major quantum number N, containing the orbital angular momenta $l = N, N-2, \ldots, 1$ or 0, then Γ equals $(N+1)(N+2)/2$.

The labels beneath the algebras in Equation (9) denote their (irreducible) representations. The nucleons are identical under $\mathrm{U}(4\Gamma)$ and therefore the representation of this algebra must be completely anti-symmetric, $[1^n] \equiv [1, \ldots, 1]$. A representation of $\mathrm{U}(s)$ is characterized by s non-negative, ordered labels $h_1 \geq h_2 \geq \cdots \geq h_s$, and therefore $[\bar{h}] \equiv [h_1, \ldots, h_\Gamma]$ and $[\bar{h}'] \equiv [h'_1, \ldots, h'_4]$. Further, since the representation of $\mathrm{U}(4\Gamma)$ is totally anti-symmetric, the representations $[\bar{h}]$ of $\mathrm{U}(\Gamma)$ and $[\bar{h}']$ of $\mathrm{U}_{ST}(4)$ must be *conjugate*; that is, their Young tableaux are obtained from each other by interchanging rows and columns.

The definition of the generators of the different algebras in terms of nucleon creation and annihilation operators can be found in Ref. [29]. Here, we just point out that the classification (9) can be replaced by an equivalent one,

$$\begin{array}{ccccc} \mathrm{U}(4\Gamma) & \supset & \mathrm{U}(\Gamma) & \otimes & \mathrm{SU}_{ST}(4) \\ \downarrow & & \downarrow & & \downarrow \\ [1^n] & & [\bar{h}] & & (\lambda, \mu, \nu) \end{array}, \tag{10}$$

where the labels (λ, μ, ν) are related as follows to $[\bar{h}']$:

$$\lambda \equiv h'_1 - h'_2, \quad \mu \equiv h'_2 - h'_3, \quad \nu \equiv h'_3 - h'_4. \tag{11}$$

A supermultiplet contains all states in a representation $[\bar{h}]$ of $\mathrm{U}(\Gamma)$ or, equivalently, in a representation (λ, μ, ν) of $\mathrm{SU}_{ST}(4)$. The basic idea of Wigner's model is that *the nucleon*–nucleon interaction favors states with maximal spatial symmetry and therefore the different supermultiplets are well separated in energy. States at low energy in the spectrum of a given nucleus have maximal spatial symmetry and are said to belong to the favoured supermultiplet.

For a nucleus with N neutrons and Z protons, the favoured supermultiplet cannot contain states with isospin less than $T = |T_z| = |N - Z|/2$. The allowed values of S and T in the representation (λ, μ, ν) are found from the branching rule

$$\begin{array}{ccccc} \mathrm{SU}_{ST}(4) & \supset & \mathrm{SU}_S(2) & \otimes & \mathrm{SU}_T(2) \\ \downarrow & & \downarrow & & \downarrow \\ (\lambda, \mu, \nu) & & S & & T \end{array}, \tag{12}$$

the Wigner coefficients of which can be obtained with general techniques [30,31]. In this way, one determines the favoured supermultiplet that is compatible with the T_z of a nucleus.

The point of interest in the present discussion is that the operator $\sigma_\mu \tau_\nu$ is a generator of the $\mathrm{SU}_{ST}(4)$ algebra and, as a consequence, GT transitions are forbidden between states belonging to different supermultiplets.

Let us further specify the orbital part U(Γ) of the classification (10). As shown by Elliott [32,33], for an entire oscillator shell [$\Gamma = (N+1)(N+2)/2$], the following generic orbital classification exists:

$$\mathrm{U}[(N+1)(N+2)/2] \supset \mathrm{SU}(3) \supset \mathrm{SO}(3). \tag{13}$$

There are, in fact, 2^{N-1} possible SU(3) subalgebras, distinguished by different phase choices in the quadrupole generator. Of particular interest for the example discussed below is the *sd* shell with $N = 2$, in which case Equation (13) reduces to

$$\mathrm{U}(6) \supset \mathrm{SU}_{\pm}(3) \supset \mathrm{SO}(3). \tag{14}$$

Two SU(3) subalgebras can be defined, differing by the relative sign of the *sd* and *dd* components of the quadrupole operator, akin to the situation in the interacting boson model (IBM) [34]. Since it turns out that the phase is of relevance for GT transitions, the two subalgebras are explicitly denoted as $\mathrm{SU}_{\pm}(3)$.

To summarize, the *n*-nucleon eigenstates of a Hamiltonian with SU(4) symmetry can be written as

$$|n(\lambda\mu\nu)\alpha LSJT\rangle, \tag{15}$$

where α denotes any remaining label necessary for a full characterization of the states in orbital space.

5. Pseudo-SU(4) Symmetry

But for the lightest nuclei, SU(4) symmetry is strongly broken mainly as a consequence of the spin–orbit interaction. In certain mass regions, however, a *pseudo*-SU(4) symmetry might be appropriate. The latter derives from the idea of pseudo-spin symmetry, which was suggested simultaneously and independently by Arima et al. [2] and by Hecht and Adler [3] and was given an explanation the context of relativistic mean-field theory [35–37]. With reference to the example discussed below, in nuclei with $28 \leq N, Z \leq 40$, this symmetry arises by treating the $1p_{1/2}$, $1p_{3/2}$ and $0f_{5/2}$ orbitals as a pseudo-*sd* shell.

A nuclear Hamiltonian with pseudo-SU(4) symmetry satisfies

$$[H, \tilde{\sigma}_\mu] = [H, \tau_\nu] = [H, \tilde{\sigma}_\mu \tau_\nu] = 0, \tag{16}$$

where $\tilde{\sigma}_\mu$ are Pauli matrices in pseudo-spin space. Since the pseudo-spin–orbit splitting (between $1p_{3/2}$ and $0f_{5/2}$ in the above example) is substantially smaller than the standard spin–orbit splitting (between $1p_{1/2}$ and $1p_{3/2}$, or between $0f_{5/2}$ and $0f_{7/2}$), the violation of the first commutator in Equation (16) is correspondingly smaller. The Hamiltonian satisfying the commutation relations (16) has eigenstates with the following labels:

$$|n(\widetilde{\lambda\mu\nu})\tilde{\alpha}\tilde{L}\tilde{S}JT\rangle, \tag{17}$$

where n is the number of nucleons in an entire pseudo-oscillator shell, $\tilde{L}$ is the total pseudo-orbital angular momentum, $\tilde{S}$ the total pseudo-spin, and $\tilde{\alpha}$ is any necessary remaining label.

In the example of the pseudo-*sd* shell, the degeneracy of the $1p_{3/2}$ and $0f_{5/2}$ orbitals is necessary but not sufficient for pseudo-SU(4) symmetry to hold since the latter requires also that the nucleon–nucleon interaction be invariant under pseudo-spin and isospin transformations. In particular, a pseudo version of SU(3) can be formulated [38,39]. More generally, it can be tested whether a realistic shell-model interaction satisfies invariance under pseudo-SU(4) and pseudo-SU(3), as was performed in Ref. [40] for $A = 58, 60$ nuclei.

The GT matrix element between the pseudo-SU(4) states (17)

$$\langle n(\widetilde{\lambda_\mathrm{f}\mu_\mathrm{f}\nu_\mathrm{f}})\tilde{\alpha}_\mathrm{f}\tilde{L}_\mathrm{f}\tilde{S}_\mathrm{f}J_\mathrm{f}T_\mathrm{f}T_{z\mathrm{f}}||\bar{\sigma}\bar{\tau}||n(\widetilde{\lambda_\mathrm{i}\mu_\mathrm{i}\nu_\mathrm{i}})\tilde{\alpha}_\mathrm{i}\tilde{L}_\mathrm{i}\tilde{S}_\mathrm{i}J_\mathrm{i}T_\mathrm{i}T_{z\mathrm{i}}\rangle, \tag{18}$$

can be rewritten as the matrix element of the transformed operator between SU(4) states (15),

$$\langle n(\lambda_f\mu_f\nu_f)\alpha_f L_f S_f J_f T_f T_{zf}||\tilde{\bar{\sigma}}\bar{\tau}||n(\lambda_i\mu_i\nu_i)\alpha_i L_i S_i J_i T_i T_{zi}\rangle. \tag{19}$$

One therefore needs to apply the pseudo-spin transformation to the GT operator. In the following we use the pseudo-spin transformation involving the r-helicity operator as defined by Bohr et al. [41]

$$\tilde{O} = O + \frac{1}{r^2}(\bar{r}\cdot\bar{\sigma})[O, \bar{r}\cdot\bar{\sigma}], \tag{20}$$

for any operator O. More general transformations can be defined [42], in particular the p-helicity transformation suggested microscopically [36,43], leading to the same expression for the GT matrix elements. The pseudo-spin transformation (20) applied to the GT operator yields

$$\tilde{\bar{\sigma}}\bar{\tau} = -\bar{\sigma}\bar{\tau} + \frac{2}{r^2}(\bar{r}\cdot\bar{\sigma})\bar{r}\bar{\tau} = -\frac{1}{3}\bar{\sigma}\bar{\tau} - \frac{4\sqrt{2\pi}}{3}[Y_2\times\bar{\sigma}]^{(1)}\bar{\tau}. \tag{21}$$

The first term is proportional to the GT operator itself and therefore follows the same selection rules. However, allowed GT transitions in pseudo-SU(4) have ft values that are about one order of magnitude larger than the corresponding ones in SU(4) due to the factor $-\frac{1}{3}$. The second term in Equation (21) introduces a *dependence on the quadrupole deformation of the nucleus*. This differs from standard SU(4), where predicted ft values are structure independent.

6. An Example: Gamow–Teller Decay of a Two-Nucleon System

We calculate GT transitions between two-nucleon states in the *sd* and pseudo-*sd* shells, applicable to the decays ^{18}Ne $\to$ ^{18}F and ^{58}Zn $\to$ ^{58}Cu, respectively. In the *sd* shell, we assume that the Hamiltonian conserves the orbital angular momentum L and the spin S, in addition to the total angular momentum J and isospin T. In the pseudo-*sd* shell, the Hamiltonian is assumed to conserve $\tilde{L}$, $\tilde{S}$, J, and T.

The B(GT) strength can be obtained with the help of Equation (7), together with the two-nucleon matrix element in an LST basis,

$$\begin{aligned}
&\langle l_1 l_2 LST||||Y_\lambda\bar{\sigma}\bar{\tau}||||l_1' l_2' L' S' T'\rangle_{\text{direct}} \\
&= \hat{L}\hat{L}'\hat{S}\hat{S}'\hat{T}\hat{T}'(-)^{l_1+l_2'+\lambda}\begin{Bmatrix} S & S' & 1 \\ 1/2 & 1/2 & 1/2\end{Bmatrix}\begin{Bmatrix} T & T' & 1 \\ 1/2 & 1/2 & 1/2\end{Bmatrix}\langle 1/2||\bar{\sigma}||1/2\rangle\langle 1/2||\bar{\tau}||1/2\rangle \\
&\times\left[(-)^{L'+S'+T'}\begin{Bmatrix} L & L' & \lambda \\ l_1' & l_1 & l_2\end{Bmatrix}\langle l_1||Y_\lambda||l_1'\rangle\delta_{l_2 l_2'} + (-)^{L+S+T}\begin{Bmatrix} L & L' & \lambda \\ l_2' & l_2 & l_1\end{Bmatrix}\langle l_2||Y_\lambda||l_2'\rangle\delta_{l_1 l_1'}\right],
\end{aligned} \tag{22}$$

where

$$\langle 1/2||\bar{\sigma}||1/2\rangle = \langle 1/2||\bar{\tau}||1/2\rangle = \sqrt{6}, \qquad \langle l||Y_\lambda||l'\rangle = (-)^l\frac{\hat{l}\hat{\lambda}\hat{l}'}{\sqrt{4\pi}}\begin{pmatrix} l & \lambda & l' \\ 0 & 0 & 0\end{pmatrix}. \tag{23}$$

The GT transition strength between anti-symmetric two-nucleon states can be obtained by taking appropriate combinations of the direct matrix element (22).

6.1. The ^{18}Ne $\to$ ^{18}F Decay

The GT transitions take place from the ground state of the parent nucleus with the structure

$$|0_1^+\rangle \equiv |L = S = J = 0, T = 1\rangle = \alpha_{001}|{}^1S_1(s^2)\rangle + \beta_{001}|{}^1S_1(d^2)\rangle, \tag{24}$$

to two possible states in the daughter nucleus

$$|1_1^+\rangle \equiv |L=0,S=J=1,T=0\rangle_1 = \alpha_{010}|\,^3S_0(s^2)\rangle + \beta_{010}|\,^3S_0(d^2)\rangle,$$
$$|1_2^+\rangle \equiv |L=0,S=J=1,T=0\rangle_2 = \beta_{010}|\,^3S_0(s^2)\rangle - \alpha_{010}|\,^3S_0(d^2)\rangle, \tag{25}$$

with $\alpha_{LST}^2 + \beta_{LST}^2 = 1$ and where the notation $^{2S+1}L_T$ is used. In round brackets are indicated the single-particle orbital angular momenta s and d, from which the coupled orbital angular momentum L is obtained. If L and S are conserved, a decay to other states in the daughter nucleus is not possible. With the expression (22), we find

$$\langle {}^3S_0(s^2)||||\bar{\sigma}\bar{\tau}||||{}^1S_1(s^2)\rangle = \langle {}^3S_0(d^2)||||\bar{\sigma}\bar{\tau}||||{}^1S_1(d^2)\rangle = -6,$$
$$\langle {}^3S_0(s^2)||||\bar{\sigma}\bar{\tau}||||{}^1S_1(d^2)\rangle = \langle {}^3S_0(d^2)||||\bar{\sigma}\bar{\tau}||||{}^1S_1(s^2)\rangle = 0, \tag{26}$$

and with the help of Equation (7) we obtain

$$B(\mathrm{GT};0_1^+ \to 1_1^+) = 6(\alpha_{001}\alpha_{010} + \beta_{001}\beta_{010})^2,$$
$$B(\mathrm{GT};0_1^+ \to 1_2^+) = 6(\alpha_{001}\beta_{010} - \beta_{001}\alpha_{010})^2. \tag{27}$$

For a Hamiltonian with SU(4) symmetry [e.g., Elliott's SU(3) model], one has $\alpha_{001} = \alpha_{010}$ and $\beta_{001} = \beta_{010}$, and all GT strength is concentrated in the 1_1^+ level. If SU(4) symmetry is broken but L and S are conserved, for example, by taking an interaction with unequal isoscalar and isovector strengths, the $B(\mathrm{GT})$ strength is distributed over two 1^+ levels. Note that, since the initial system has no neutrons, $S^- = 0$, and the Ikeda sum rule (3) is satisfied.

6.2. The ^{58}Zn $\to$ ^{58}Cu *Decay*

As explained in Section 5 the calculation of GT transitions in a pseudo-*sd* shell can be replaced by one in the *sd* shell with the transformed GT operator $\tilde{\sigma}\bar{\tau}$ of Equation (21). With the latter operator transitions take place from the ground state (24) of the parent nucleus to five possible states in the daughter nucleus, namely to the two 1^+ states (25) and to

$$|1_3^+\rangle \equiv |L=2,S=J=1,T=0\rangle_1 = \alpha_{210}|\,^3D_0(sd)\rangle + \beta_{210}|\,^3D_0(d^2)\rangle,$$
$$|1_4^+\rangle \equiv |L=2,S=J=1,T=0\rangle_2 = \beta_{210}|\,^3D_0(sd)\rangle - \alpha_{210}|\,^3D_0(d^2)\rangle,$$
$$|1_5^+\rangle \equiv |L=2,S=J=1,T=1\rangle = |\,^3D_1(sd)\rangle. \tag{28}$$

Note that a GT transition to a $T = 1$ state is allowed. The first piece of the transformed GT operator (21) is proportional to $\bar{\sigma}\bar{\tau}$, for which we use the expression (26). The matrix elements of $Y_2\bar{\sigma}\bar{\tau}$ are obtained from Equation (22)

$$\langle {}^3D_0(sd)||||Y_2\bar{\sigma}\bar{\tau}||||{}^1S_1(s^2)\rangle = -\sqrt{\frac{45}{2\pi}}, \quad \langle {}^3D_0(d^2)||||Y_2\bar{\sigma}\bar{\tau}||||{}^1S_1(s^2)\rangle = 0,$$
$$\langle {}^3D_0(sd)||||Y_2\bar{\sigma}\bar{\tau}||||{}^1S_1(d^2)\rangle = -\sqrt{\frac{9}{2\pi}}, \quad \langle {}^3D_1(d^2)||||Y_2\bar{\sigma}\bar{\tau}||||{}^1S_1(d^2)\rangle = \sqrt{\frac{90}{7\pi}},$$
$$\langle {}^3D_1(sd)||||Y_2\bar{\sigma}\bar{\tau}||||{}^1S_1(s^2)\rangle = -\sqrt{\frac{45}{\pi}}, \quad \langle {}^3D_1(sd)||||Y_2\bar{\sigma}\bar{\tau}||||{}^1S_1(d^2)\rangle = \sqrt{\frac{9}{\pi}}, \tag{29}$$

leading to

$$
\begin{aligned}
B(\mathrm{GT};0_1^+ \to 1_1^+) &= \frac{2}{3}(\alpha_{001}\alpha_{010} + \beta_{001}\beta_{010})^2,\\
B(\mathrm{GT};0_1^+ \to 1_2^+) &= \frac{2}{3}(\alpha_{001}\beta_{010} - \beta_{001}\alpha_{010})^2,\\
B(\mathrm{GT};0_1^+ \to 1_3^+) &= \frac{8}{105}(\sqrt{35}\alpha_{001}\alpha_{210} + \sqrt{7}\beta_{001}\alpha_{210} - \sqrt{20}\beta_{001}\beta_{210})^2,\\
B(\mathrm{GT};0_1^+ \to 1_4^+) &= \frac{8}{105}(\sqrt{35}\alpha_{001}\beta_{210} + \sqrt{7}\beta_{001}\beta_{210} + \sqrt{20}\beta_{001}\alpha_{210})^2,\\
B(\mathrm{GT};0_1^+ \to 1_5^+) &= \frac{4}{15}(\sqrt{10}\alpha_{001} - \sqrt{2}\beta_{001})^2.
\end{aligned} \tag{30}
$$

We now apply these expressions to the SU(3) limits of the pseudo-*sd* shell, for which the coefficients α_{LST} and β_{LST} are listed in Table 1. Note that $\mathrm{SU}_-(3)$ and $\mathrm{SU}_+(3)$, corresponding to prolate and oblate shapes, respectively, differ by just a sign in one of the coefficients. The Gamow–Teller strengths $B(\mathrm{GT};0_1^+ \to 1_i^+)$ obtained after inserting the coefficients of Table 1 in Equation (30) are shown in Table 2. The total strength given by the Ikeda sum rule (remember that $S^- = 0$) is not found in the SU(3) limits. The reason is that a fraction of the ground-state wave function corresponds to two protons in the $0f_{5/2}$ orbital and the total Ikeda sum rule can only be recovered if the model space includes the $0f_{7/2}$ orbital, which is absent from the pseudo-*sd* shell. The same fraction $\frac{502}{105} \approx 4.781$ is found in $\mathrm{SU}_-(3)$ and $\mathrm{SU}_+(3)$, but the strength is differently distributed in the two limits, indicating the impact of the shape of the nucleus on the B(GT) distribution. This simple analysis therefore confirms the original proposal of Hamamoto and Zhang [44] that the distribution of GT strength depends on the shape of the nucleus, a result later confirmed in several nuclei theoretically [45,46] and based on theoretical calculations, experimentally [47–52].

Table 1. The coefficients α_{LST} and β_{LST} of the expansions (24), (25), (28) in the SU(3) limits of the *sd* shell.

	α_{001}	β_{001}	α_{010}	β_{010}	α_{210}	β_{210}
$\mathrm{SU}_-(3)$	$\sqrt{\frac{5}{9}}$	$\sqrt{\frac{4}{9}}$	$\sqrt{\frac{5}{9}}$	$\sqrt{\frac{4}{9}}$	$\sqrt{\frac{7}{9}}$	$\sqrt{\frac{2}{9}}$
$\mathrm{SU}_+(3)$	$\sqrt{\frac{5}{9}}$	$\sqrt{\frac{4}{9}}$	$\sqrt{\frac{5}{9}}$	$\sqrt{\frac{4}{9}}$	$\sqrt{\frac{7}{9}}$	$-\sqrt{\frac{2}{9}}$

Table 2. Gamow–Teller strengths $B(\mathrm{GT};0_1^+ \to 1_i^+)$ in the SU(3) limits of the pseudo-*sd* shell.

	$0_1^+ \to 1_1^+$	$0_1^+ \to 1_2^+$	$0_1^+ \to 1_3^+$	$0_1^+ \to 1_4^+$	$0_1^+ \to 1_5^+$
$\mathrm{SU}_-(3)$	0.667	0	1.243	2.338	0.533
$\mathrm{SU}_+(3)$	0.667	0	3.575	0.006	0.533

We conclude this illustrative example with the remark that identical results are obtained with the standard Gamow–Teller operator $\bar{\sigma}\bar{\tau}$ acting in the model space formed by the $1p_{1/2}$, $1p_{3/2}$ and $0f_{5/2}$ orbitals, a calculation which then necessarily must be carried out in *jj* coupling.

7. Gamow–Teller Decay of $58 \leq A \leq 70$ Nuclei

In order to extend the preceding results to nuclei with more valence nucleons, we consider the following schematic Hamiltonian:

$$
H = \epsilon_{\tilde{s}} n_{\tilde{s}} - 4\pi \sum_{T=0,1} a'_T \sum_{i<j} \delta(\bar{r}_i - \bar{r}_j)\delta(r_i - R_0) - \sum_{\pm} \kappa_{\pm}(Q_{\pm} \cdot Q_{\pm} + 3L \cdot L), \tag{31}
$$

which depends on the five parameters $\epsilon_{\tilde{s}}$, a_0, a_1, κ_-, and κ_+. We choose the $\tilde{d}$ orbitals $1p_{3/2}$ and $0f_{5/2}$ at zero energy and put the $\tilde{s}$ orbital $1p_{1/2}$ at an energy $\epsilon_{\tilde{s}}$. The coefficients

$a_T \equiv a'_T C(R_0)$ (where $C(R_0)$ is a radial integral) determine the strengths of the surface delta interaction (SDI) in the isoscalar ($T = 0$) and isovector ($T = 1$) channels. The parameters $\kappa_\pm$ are the strengths of the quadrupole interaction, where κ_- (κ_+) corresponds to prolate (oblate) deformation. The term $3L \cdot L$ is added such that, in combination with $Q_\pm \cdot Q_\pm$, the sum of the two terms is proportional to the quadratic Casimir operator of $SU_\pm(3)$. Signs in the Hamiltonian (31) are chosen such that all parameters are positive. The Hamiltonian (31) clearly is of a schematic nature and one cannot expect to obtain with it a detailed reproduction of the data. The purpose of the present exercise is rather to arrive at an intuitive understanding how the B(GT) distribution depends on the different terms.

We first study the dependence of the B(GT) distributions on the character of the quadrupole deformation. In Figure 5 is shown the calculated GT strength in the decay $(N = Z - 2) \rightarrow (N = Z)$ for $A = 58$, 62, 66, and 70, in three typical cases, namely no quadrupole deformation ($\kappa_\pm = 0$), prolate ($\kappa_- = 20$ keV), or oblate ($\kappa_+ = 20$ keV) deformation. For ease of comparison, other parameters are kept fixed, $\epsilon_{\tilde{s}} = 0$, $a_0 = 0.5$ and $a_1 = 0.6$ MeV. A standard GT quenching of $q^2 = 0.74^2$ is applied. The distribution calculated for $A = 58$ confirms the result of the previous section in the pseudo-$SU_\pm(3)$ limits since for prolate deformation the GT strength is pushed to higher excitation energy. For higher mass numbers A, however, this simple SU(3) picture is altered by the SDI: it is rather in the case of oblate deformation that GT strength is found at higher excitation energy. The distributions for $A = 66$ and $A = 70$ are exactly the same since for $\epsilon_{\tilde{s}} = 0$ the Hamiltonian (31) has particle–hole symmetry.

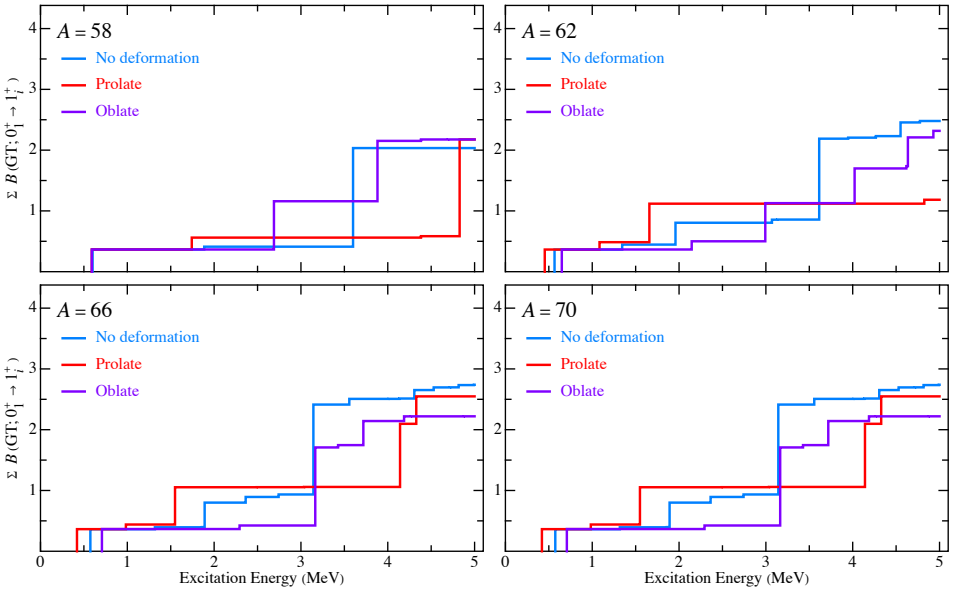

Figure 5. Distributions of the GT strength in the decay from $N = Z - 2$ to $N = Z$ nuclei for $A = 58$, 62, 66, and 70, and its dependence on the quadrupole deformation. The Hamiltonian (31) is used with $\epsilon_{\tilde{s}} = 0$. The quadrupole deformation is either zero ($\kappa_\pm = 0$, blue), prolate ($\kappa_- = 20$ keV, red), or oblate ($\kappa_+ = 20$ keV, purple). The parameters of the SDI are $a_0 = 0.5$ and $a_1 = 0.6$ MeV, and the GT strength is calculated with a quenching factor $q^2 = 0.74^2$.

To compare with the observed B(GT) distributions, some empirical procedure should be followed to obtain the parameters in the Hamiltonian (31). There is only a weak dependence of the GT strength on $\epsilon_{\tilde{s}}$, which is taken constant, $\epsilon_{\tilde{s}} = 1$ MeV. In contrast, the parameters of the SDI do strongly impact the B(GT) distributions. They can be determined from two experimental properties, namely the difference $\Delta E_2 \equiv E(2_1^+) - E(0_1^+)$ in the parent (or in its mirror nucleus) and the difference $\Delta E_1 \equiv E(1_1^+) - E(0_1^+)$ in the daughter. Given the quadrupole moment $Q(2_1^+) = -0.10(6)$ in ^{58}Ni [53], a weak prolate deformation is taken for $A = 58$. Little is known of the deformation in the heavier nuclei, and we have

assumed that the deformation remains weakly prolate from ^{62}Ga to ^{70}Br. It should be noted, however, that the small GT strength observed at low energy for $A = 62$ and 66 seems to favor an oblate deformation. This procedure leads to the parameters given in Table 3. The calculated B(GT) distributions obtained with the parameters of Table 3 are compared with the experimental ones in Figure 6.

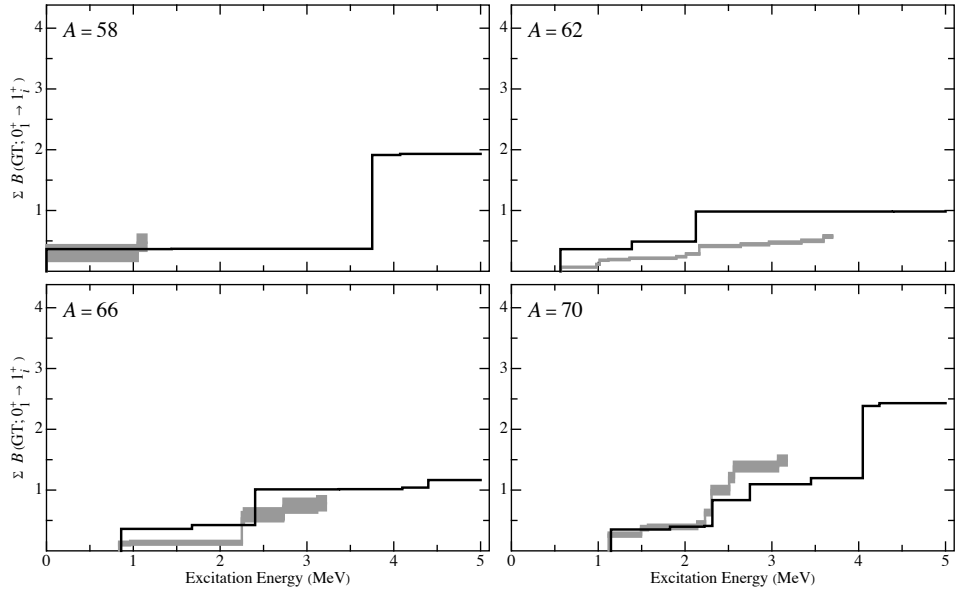

Figure 6. Distributions of the GT strength in the decay from $N = Z - 2$ to $N = Z$ nuclei for $A = 58$, 62, 66, and 70. The experimental B(GT) distributions and their uncertainties are indicated in grey. Parameters of the Hamiltonian (31) are given in Table 3 and the GT strength is calculated with a quenching factor $q^2 = 0.74^2$.

Table 3. Parameters (in keV) of the Hamiltonian (31) together with the experimental (ex) and calculated (th) energy differences ΔE_2 and ΔE_1 (see text) for $A = 58$, 62, 66, and 70.

A	$\epsilon_{\tilde{s}}$	a_0	a_1	κ_-	κ_+	$\Delta E_{2,\mathrm{ex}}$	$\Delta E_{2,\mathrm{th}}$	$\Delta E_{1,\mathrm{ex}}$	$\Delta E_{1,\mathrm{th}}$
58	1000	500	470	10	0	1356	1363	−203	−178
62	1000	600	710	10	0	954	936	571	564
66	1000	640	820	10	0	957	949	837	860
70	1000	480	700	10	0	945	907	1120	1147

It should be emphasised that the GT strength is sensitively dependent on several parameters in the schematic Hamiltonian (31), and hence no firm conclusion can be drawn on the question whether a prolate or an oblate deformation agrees better with experiment. Nevertheless, one feature in the calculated distributions, namely the GT strength to the first 1^+ level, is largely independent of the detailed structure of the Hamiltonian. Insight into this result can be obtained with reference to the transformed GT operator (21). The first piece of the transformed operator, $-\frac{1}{3}\bar{\sigma}\bar{\tau}$, is responsible for GT strength towards the 1^+_1 level. Since $a_0 \neq a_1$, the SU(4) symmetry is broken, but this breaking is so small that the $\Delta L = 0$ GT strength is mainly concentrated in 1^+_1. Because of the factor $\frac{1}{3}$ in the transformed operator, the predicted strength is one-ninth of the SU(4) value, that is, $B(\mathrm{GT}; 0^+_1 \to 1^+_1) \approx \frac{2}{3}q^2$. In contrast, the distribution of the $\Delta L = 2$ strength at higher excitation energy generated by the second piece of the transformed operator, $-\frac{4\sqrt{2\pi}}{3}[Y_2 \times \bar{\sigma}]^{(1)}\bar{\tau}$, is strongly influenced by the values of a_0 and a_1 and their interplay with the strength of the quadrupole force.

It is seen from Figure 6 that the calculated $B(\mathrm{GT}; 0^+_1 \to 1^+_1)$ value agrees with experiment for $A = 58$. This is one of the arguments to propose the existence of a pseudo-SU(4) symmetry in ^{58}Cu [40]. On the other hand, the calculated $B(\mathrm{GT}; 0^+_1 \to 1^+_1)$ value in $A = 62$

and 66 is much larger than what is observed. Given that $B(\mathrm{GT}; 0_1^+ \to 1_1^+) \approx \frac{2}{3}q^2$ is a robust prediction of pseudo-SU(4), one is led to conclude that this symmetry is absent from ^{62}Ga and ^{66}As. By the same token, the experimentally observed GT strength in $A = 70$ indicates a restoration pseudo-SU(4) symmetry in ^{70}Br.

8. Conclusions

In this contribution, a review was given of the properties of Gamow–Teller (GT) transitions in the nuclear shell model under the assumption of SU(4) or pseudo-SU(4) symmetry. Since the GT transition operator is a generator of the SU(4) algebra, SU(4) symmetry gives rise to selection rules in β decay. These are approximately observed in light nuclei but strongly broken in heavier ones. Nevertheless, a symmetry-based analysis of GT strength can still be carried out by assuming a nuclear Hamiltonian with pseudo-SU(4) rather than SU(4) symmetry. The main outcome of the latter analysis is the observation of a dependence of GT strength on the shape of the nucleus, thus confirming from a symmetry perspective the study of Hamamoto and Zhang [44], who derived the same result in a mean-field approach. However, schematic calculations show that other terms in a nuclear Hamiltonian with pseudo-SU(4) symmetry also strongly influence the distribution of GT strength. Therefore, the connection between the shape of the nucleus (i.e., prolate or oblate) and the distribution of GT strength is not a straightforward one.

SU(4) symmetry dictates that most of the GT strength from the ground state of a $Z = N + 2$ parent nucleus is concentrated in the yrast $J^\pi = 1^+$ state of the $N = Z$ daughter nucleus. This property is no longer valid for a Hamiltonian with pseudo-SU(4) symmetry, in which case the GT strength can go to many $J^\pi = 1^+$ states with a distribution that intricately depends on several parameters in the Hamiltonian. Nevertheless, one robust property, largely independent of parameters, survives in pseudo-SU(4): the yrast $J^\pi = 1^+$ state collects about one-ninth of the strength expected in SU(4), $B(\mathrm{GT}; 0_1^+ \to 1_1^+) \approx \frac{2}{3}q^2$, where q is the GT quenching factor. The observed GT strength in the $^{58}\mathrm{Zn} \to {}^{58}\mathrm{Cu}$ decay is consistent with this prediction and therefore supports the existence of a pseudo-SU(4) symmetry in the $A = 58$ nuclei. GT strength in support of pseudo-SU(4) symmetry is also found in the $^{70}\mathrm{Kr} \to {}^{70}\mathrm{Br}$ decay but not in the $^{62}\mathrm{Ge} \to {}^{62}\mathrm{Ga}$ and $^{66}\mathrm{Se} \to {}^{66}\mathrm{As}$ decays. On the basis of these observations, one can therefore conjecture a restoration of pseudo-SU(4) symmetry in the $A = 70$ nuclei.

Author Contributions: Data curation, P.V.I., A.A., A.V.-S., G.G.K., S.E.A.O., B.R. and P.A.; Funding acquisition, A.A., G.G.K. and B.R.; Investigation, P.V.I., A.A., A.V.-S., G.G.K., S.E.A.O., B.R. and P.A.; Methodology, P.V.I.; Writing—original draft, P.V.I., A.A., A.V.-S., G.G.K., S.E.A.O., B.R. and P.A.; Writing—review & editing, P.V.I., A.A., A.V.-S., G.G.K., S.E.A.O., B.R. and P.A. All authors have read and agreed to the published version of the manuscript.

Funding: This work was supported by the Spanish Ministerio de Ciencia e Inno-vacion Grants No. PID2019-104714GB-C21, PID2022-138297NB-C21, Generalitat Valenciana Grants No. PROMETEO/2019/007, CIPROM/2022/9. B. R. y P.A acknowledges the CSIC cooperation grant COOP20125, A. A. acknowledges partial support of the JSPS Invitational Fellowships for Research in Japan (ID: L1955) This work was supported by the National Research, Development, and Innovation Fund of Hungary, financed under the K18 funding scheme (Projects No. NN128072 and K128729).

Institutional Review Board Statement: Not applicable.

Informed Consent Statement: Not applicable.

Data Availability Statement: Data available on request.

Acknowledgments: The experimental work was carried out at GANIL and at RIBF. RIBF is operated by RIKEN Nishina Center and CNS, University of Tokyo. We acknowledge the EUROBALL Owners Committee for the loan of germanium detectors and the PreSpec Collaboration for the read-out electronics of the cluster detectors. We also acknowledge the contribution of many colleagues that helped in the realization of the experiments.

Conflicts of Interest: The authors declare no conflict of interest.

Abbreviations

The following abbreviations are used in this manuscript:

GANIL	Grand Accélérateur National d'Ions Lourds
GSI	GSI Helmholtzzentrum für Schwerionenforschung
GT	Gamow–Teller
RIKEN	Rikagaku Kenkyüjyo
SDI	surface delta interaction

References

1. Wigner, E. On the consequences of the symmetry of the nuclear hamiltonian on the spectroscopy of nuclei. *Phys. Rev.* **1937**, *51*, 106–119. [CrossRef]
2. Arima, A.; Harvey, M.; Shimizu, K. Pseudo *LS* coupling and pseudo SU_3 coupling schemes. *Phys. Lett. B* **1969**, *30*, 517–522. [CrossRef]
3. Hecht, K.T.; Adler, A. Generalized seniority for favored $J \neq 0$ pairs in mixed configurations. *Nucl. Phys. A* **1969**, *137*, 129–143. [CrossRef]
4. GANIL. Available online: https://www.ganil-spiral2.eu (accessed on 27 July 2023).
5. GSI. Available online: https://www.gsi.de/start/aktuelles (accessed on 27 July 2023).
6. RIKEN. Available online: https://www.nishina.riken.jp/index_e.html (accessed on 27 July 2023).
7. Wallace, R.K.; Woosley, S.E. Explosive hydrogen burning. *Astrophys. J. Suppl.* **1981**, *45*, 389–422. [CrossRef]
8. Schatz, H.; Aprahamian, A.; Barnard, V.; Bildsten, L.; Cumming, A.; Ouellette, M.; Rauscher, T.; Thielemann, F.K.; Wiescher, M. End Point of the rp Process on Accreting Neutron Stars. *Phys. Rev. Lett.* **2001**, *86*, 3471–3474. [CrossRef] [PubMed]
9. Kucuk, L.; Orrigo, S.E.A.; Montaner-Pizá, A.; Rubio, B.; Fujita, Y.; Gelletly, W.; Blank, B.; Oktem, Y.; Adachi, T.; Algora, A.; et al. Half-life determination of $Tz = -1$ and $Tz = -1/2$ proton-rich nuclei and the β decay of ^{58}Zn. *Eur. Phys. J. A* **2017**, *53*, 134-1–134-10. [CrossRef]
10. Anne, R.; Mueller, A.C. LISE 3: A magnetic spectrometer-Wien filter combination for secondary radioactive beam production. *Nucl. Instrum. Methods Phys. Res. B* **1992**, *70*, 276–285. [CrossRef]
11. Colourful Nuclide Chart. Available online: https://people.physics.anu.edu.au/~ecs103/chart/ (accessed on 3 July 2023).
12. Fukuda, N.; Kubo, T.; Ohnishi, T.; Inabe, N.; Takeda, H.; Kameda, D.; Suzuki, H. Identification and separation of radioactive isotope beams by the BigRIPS separator at the RIKEN RI Beam Factory. *Nucl. Instrum. Methods B* **2013**, *317*, 323–332. [CrossRef]
13. Nishimura, S. Beta-gamma spectroscopy at RIBF. *Prog. Theor. Exp. Phys.* **2012**, *2012*, 03C006. [CrossRef]
14. Söderström, P.-A.; Nishimura, S.; Doornenbal, P.; Lorusso, G.; Sumikama, T.; Watanabe, H.; Xu, Z.Y.; Baba, H.; Browne, F.; Go, S.; et al. Installation and commissioning of EURICA—Euroball-RIKEN Cluster Array. *Nucl. Instrum. Methods B* **2013**, *317*, 649–652. [CrossRef]
15. Grodner, E.; Gadea, A.; Sarriguren, P.; Lenzi, S.M.; Grebosz, J.; Valiente-Dobón, J.J.; Algora, A.; Górska, M.; Regan, P.H.; Rudolph, D.; et al. Hindered Gamow-Teller decay to the odd–odd $N = Z$ ^{62}Ga: Absence of proton-neutron $T = 0$ condensate in $A = 62$. *Phys. Rev. Lett.* **2014**, *113*, 092501-1–092501-5. [CrossRef]
16. Orrigo, S.E.A.; Rubio, B.; Gelletly, W.; Aguilera, P.; Algora, A.; Morales, A.I.; Agramunt, J.; Ahn, D.S.; Ascher, P.; Blank, B.; et al. β decay of the very neutron-deficient ^{60}Ge and ^{62}Ge nuclei. *Phys. Rev. C* **2021**, *103*, 014324-1–014324-12. [CrossRef]
17. Lopéz Jiménez, M.J.; Blank, B.; Chartier, M.; Czajkowski, S.; Dessagne, P.; De France, G.; Giovinazzo, J.; Karamanis, D.; Lewitowicz, M.; Maslov, V.; et al. Half-life measurements of proton-rich ^{78}Kr fragments. *Phys. Rev. C* **2002**, *66*, 025803-1–025803-8. [CrossRef]
18. Aguilera, P. *Manuscript in Preparation*; Dipartimento di Fisica e Astronomia, Università degli Studi di Padova: Padova, Italy, 2023.
19. Aguilera, P. Study of Gamow-Teller transitions of $T_z = -2$ ^{64}Se and $T_z = -1$ ^{66}Se. Ph.D. Thesis, University of Chile, Santiago, Chile, 2020.
20. Vitéz-Sveiczer, A.; Algora, A.; Morales, A.I.; Rubio, B.; Kiss, G.G.; Sarriguren, P.; Van Isacker, P.; De Angelis, G.; Recchia, F.; Nishimura, S.; et al. The β-decay of ^{70}Kr into ^{70}Br: Restoration of the pseudo-SU(4) symmetry. *Phys. Lett. B* **2022**, *830*, 137123-1–137123-8. [CrossRef]
21. Jenkins, D.G.; Kelsall, N.S.; Lister, C.J.; Balamuth, D.P.; Carpenter, M.P.; Sienko, T.A.; Fischer, S.M.; Clark, R.M.; Fallon, P.; Görgen, A.; et al. $T = 0$ and $T = 1$ states in the odd–odd $N = Z$ nucleus, ^{70}Br. *Phys. Rev. C* **2002**, *65*, 064307-1–064307-16. [CrossRef]
22. Nichols, A.J.; Wadsworth, R.; Iwasaki, H.; Kaneko, K.; Lemasson, A.; De Angelis, G.; Bader, V.M.; Baugher, T.; Bazin, D.; Bentley, M.A.; et al. Collectivity in $A \sim 70$ nuclei studied via lifetime measurements in ^{70}Br and ^{68,70}Se. *Phys. Lett. B* **2014**, *733*, 52–57. [CrossRef]
23. Warburton, E.K.; Weneser, J. (Eds.) *Isospin in Nuclear Physics*; North-Holland Publishing Company: Amsterdam, The Netherlands , 1969; Chapter 5, p. 185, ISBN 7204 0155 0.
24. Molina, F.; Rubio, B.; Fujita, Y.; Gelletly, W.; Agramunt, J.; Algora, A.; Benlliure, J.; Boutachkov, P.; Cáceres, L.; Cakirli, R.B.; et al. $T_z = -1 \rightarrow \beta$ decays of ^{54}Ni, ^{50}Fe, ^{46}Cr, and ^{42}Ti and comparison with mirror (3He,t) measurements. *Phys. Rev. C* **2015**, *91*, 014301-1–014301-19. [CrossRef]
25. MacFarlane, M.H. Gamow–Teller sum rules and ground-state correlations. *Phys. Lett. B* **1986**, *182*, 265–268. [CrossRef]
26. Ikeda, K. Collective excitations of unlike pair states in heavier nuclei. *Prog. Theor. Phys.* **1964**, *31*, 434–451. [CrossRef]

27. Talmi, I. *Simple Models of Complex Nuclei. The Shell Model and the Interacting Boson Model*; Harwood: Chur, Switzerland, 1993.
28. Fujita, Y.; Rubio, B.; Gelletly, W. Spin–isospin excitations probed by strong, weak and electro-magnetic interactions. *Progr. Part. Nucl. Phys.* **2011**, *66*, 549–606. [CrossRef]
29. Van Isacker, P.; Pittel, S. Symmetries and deformations in the spherical shell model. *Phys. Scr.* **2016**, *91*, 023009-1–023009-23. [CrossRef]
30. Hecht, K.T.; Pang, S.C. On the Wigner supermultiplet scheme. *J. Math. Phys.* **1969**, *10*, 1571–1616. [CrossRef]
31. Pan, F.; Dai, L.; Draayer, J.P. Wigner coefficients of $\mathrm{U}(4) \supset \mathrm{SU}_S(2) \otimes \mathrm{SU}_T(2)$. *Nucl. Phys. A* **2023**, *1040*, 122746-1–122746-38.
32. Elliott, J.P. Collective motion in the nuclear shell model I. Classification schemes for states of mixed configurations. *Proc. Roy. Soc. A* **1958**, *245*, 128–145.
33. Elliott, J.P. Collective motion in the nuclear shell model II. The introduction of intrinsic wave-functions. *Proc. Roy. Soc. A* **1958**, *245*, 562–581.
34. Iachello, F.; Arima, A. *The Interacting Boson Model*; Cambridge University Press: Cambridge, UK, 1987.
35. Bahri, C.; Draayer, J.P.; Moszkowski, S.A. Pseudospin symmetry in nuclear physics. *Phys. Rev. Lett.* **1992**, *68*, 2133–2136. [CrossRef] [PubMed]
36. Ginocchio, J.N. Pseudospin as a relativistic symmetry. *Phys. Rev. Lett.* **1997**, *78*, 436–439. [CrossRef]
37. Ginocchio, J.N; Leviatan, A. On the relativistic foundations of pseudospin symmetry in nuclei. *Phys. Lett. B* **1998**, *425*, 1–5. [CrossRef]
38. Strottman, D. On the validity of the pseudo SU(3) for $A = 59$ and 60. *Nucl. Phys. A* **1972**, *188*, 488–512. [CrossRef]
39. Ratna Raju, R.D.; Draayer, J.P.; Hecht, K.T. Search for a coupling scheme in heavy deformed nuclei: The pseudo SU(3) model. *Nucl. Phys. A* **1973**, *202*, 433–466. [CrossRef]
40. Van Isacker, P.; Juillet, O.; Nowacki, F. Pseudo-SU(4) symmetry in pf-shell nuclei. *Phys. Rev. Lett.* **1999**, *82*, 2060–2063. [CrossRef]
41. Bohr, A.; Hamamoto, I.; Mottelson, B.R. Pseudospin in rotating nuclear potentials. *Phys. Scr.* **1982**, *26*, 267–272. [CrossRef]
42. Castaños, O.; Moshinsky, M.; Quesne, C. Transformation to pseudo-SU(3) in heavy deformed nuclei. *Phys. Lett. B* **1992**, *277*, 238–242. [CrossRef]
43. Blokhin, A.L.; Bahri, C.; Draayer, J.P. Origin of pseudospin symmetry. *Phys. Rev. Lett.* **1995**, *74*, 4149–4152. [CrossRef] [PubMed]
44. Hamamoto, I.; Zhang, X.Z. Dependence of Gamow–Teller β^+-decay of ^{80}Zr, ^{76}Sr and ^{71}Kr on nuclear shape. *Z. Phys. A* **1995**, *353*, 145–148. [CrossRef]
45. Sarriguren, P.; Moya de Guerra, E.; Escuderos, A.; Carrizo, A.C. β decay and shape isomerism in ^{74}Kr. *Nucl. Phys. A* **1998**, *635*, 55–85. [CrossRef]
46. Sarriguren, P.; Moya de Guerra, E.; Escuderos, A. Shapes and β-decay in proton rich Ge, Se, Kr and Sr isotopes. *Nucl. Phys. A* **1999**, *658*, 13–44. [CrossRef]
47. Poirier, E.; Maréchal, F.; Dessagne, P.; Algora, A.; Borge, M.J.G.; Cano-Ott, D.; Caspar, J.C.; Courtin, S.; Devin, J.; Fraile, L.M.; et al. B(GT) strength from β-decay measurements and inferred shape mixing in ^{74}Kr. *Phys. Rev. C* **2004**, *69*, 034307-1–034307-8. [CrossRef]
48. Nacher, E.; Algora, A.; Rubio, B.; Taın, J.L.; Cano-Ott, D.; Courtin, S.; Dessagne, P.; Maréchal, F.; Miehé, C.; Poirier, E.; et al. Deformation of the $N = Z$ Nucleus ^{76}Sr using β-Decay Studies. *Phys. Rev. Lett.* **2004**, *92*, 232501-1–232501-4. [CrossRef]
49. Perez-Cerdan, A.B.; Rubio, B.; Gelletly, W.; Algora, A.; Agramunt, J.; Nácher, E.; Taín, J.L.; Sarriguren, P.; Fraile, L.M.; Borge, M.J.G.; et al. Deformation of Sr and Rb isotopes close to the $N = Z$ line via β-decay studies using the total absorption technique. *Phys. Rev. C* **2013**, *88*, 014324-1–014324-15. [CrossRef]
50. Estevez Aguado, M.E.; Agramunt, J.; Rubio, B.; Taín, J.L.; Jordán Fraile, L.M.D.; Gelletly, W.; Frank, A.; Csatlós, M. Shapes of ^{192,190}Pb ground states from β-decay studies using the total-absorption technique. *Phys. Rev. C* **2015**, *92*, 044321-1–044321-8. [CrossRef]
51. Briz, J.A.; Nácher, E.; Borge, M.J.G.; Algora, A.; Rubio, B.; Dessagne, P.; Maira, A.; Cano-Ott, D.; Courtin, S.; Escrig, D.; et al. Shape study of the $N = Z$ nucleus ^{72}Kr via β decay. *Phys. Rev. C* **2015**, *92*, 054326-1–054326-10. [CrossRef]
52. Algora, A.; Ganioğlu, E.; Sarriguren, P.; Guadilla, V.; Fraile, L.M.; Nácher, E.; Rubio, B.; Taín, J.L.; Agramunt, J.; Gelletly, W.; et al. Total absorption gamma-ray spectroscopy study of the β-decay of ^{186}Hg. *Phys. Lett. B* **2021**, *819*, 136438-1–136438-7. [CrossRef]
53. Nesaraja, C.D.; Geraedts, S.D.; Singh, B. Nuclear Data Sheets for $A = 58$. *Nucl. Data Sheets* **2010**, *111*, 897–1092. [CrossRef]